Microfluidic electrospinning of biphasic nanofibers with Janus morphology

Yasmin Srivastava,[1] Manuel Marquez,[2,3] and Todd Thorsen[1,a)]
[1]*Department of Mechanical Engineering, Massachusetts Institute of Technology, Cambridge, Massachusetts 02139-4307, USA*
[2]*NIST Center for Theoretical and Computational Nanosciences, Gaithersburg, Maryland 20899, USA*
[3]*Harrington Department Bioengineering, Arizona State University, Tempe, Arizona 85287, USA*

(Received 13 August 2008; accepted 1 October 2008; published online 7 January 2009)

In this paper a method of electrospinning conducting and nonconducting biphasic Janus nanofibers using microfluidic polydimethylsiloxane (PDMS)-based manifolds is described. Key benefits of using microfluidic devices for nanofiber synthesis include rapid prototyping, ease of fabrication, and the ability to spin multiple Janus fibers in parallel through arrays of individual microchannels. Biphasic Janus nanofibers of polyvinylpyrrolidone (PVP)+polypyrrole (PPy)/PVP nanofibers with an average diameter of 250 nm were successfully fabricated using elastomeric microfluidic devices. Fiber characterization and confirmation of the Janus morphology was subsequently carried out using a combination of scanning electron microscopy, energy dispersion spectroscopy, and transmission electron microscopy. © *2009 American Institute of Physics.* [DOI: 10.1063/1.3009288]

INTRODUCTION

The demand for next generation devices and circuitries has fueled the growth of nanoscience and technology. To address this demand, researchers have turned to the development of fabrication methods not only to synthesize nanoscale building blocks, but also achieve controlled assemblies of these structural units into functional architectures. One particularly interesting area of research is the synthesis of particles from two heterogeneous materials, producing a composite whose surface chemical composition differs on two sides of the particle. This biphasic side-by-side morphology has often been referred to as "Janus," in reference to the two-headed god in Roman mythology with opposing faces.[1] To date, an impressive number of methods have been developed to fabricate Janus particles.[2–6] Examples of Janus particle synthesis methods include coelectrospraying polymeric precursors,[5] sputtering of gold onto the top face of a polymer bead array,[7] and the derivitization of beads trapped in the surface of a hydrocolloid matrix.[8] Additionally, microfluidic flow systems have been used to prepare amphiphilic particles by the polymerization of the Janus droplets formed within the microfluidic channels.[9,10]

While a significant amount of research has been reported on the development of biphasic Janus nanoparticles and microparticles, there are very few examples of the synthesis of Janus-type fibers. Janus fibers have potential attractive applications in areas such as tissue engineering, where the surface chemistries of the fibers could be applied to the design of smart scaffolds for the selective coculture of multiple cell types, and as chemical or electrical sensors, combining conductive and nonconductive polymers to fabricate materials that interface with digital readouts. Early efforts in the synthesis of composite and Janus-type nanofibers have been dominated by electrospinning methods. In a typical electrospinning process, a high voltage is applied to create electrically charged jets of a polymer solution. The charged jet then undergoes bending instability,

a)Electronic mail: thorsen@mit.edu.

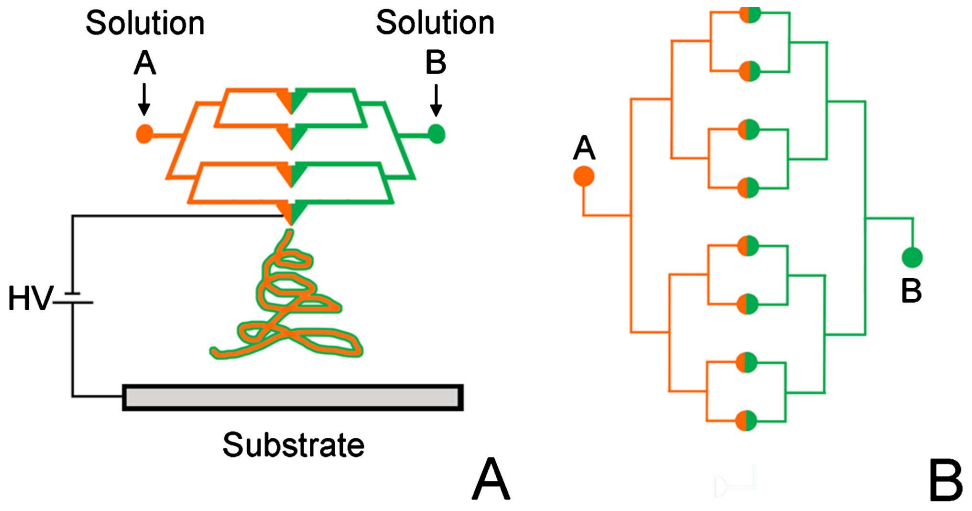

FIG. 1. (a) Schematic representation of the electrospinning setup using PDMS microfluidic device source for parallel spinning of biphasic Janus type nanofibers. (b) Layout of the channel geometry illustrating the dual microchannel architecture and connection ports to feed the solution A (PVP) and solution B (PVP+pyrrole+$FeCl_3$).

often referred to as whipping instability, stretching itself to form nanofibers, which on solvent evaporation are collected on a target as a nonwoven mat. Electrospinning has been applied to the synthesis of a wide variety of nanofiber types, ranging from single-phase polymer solutions and blends to composites containing insoluble materials such as magnetic nanoparticles.[11] Several research groups have reported the synthesis of core-sheath bicomponent nanofibers using coaxial electrospinning.[12–17] Although there are a few reports on side-by-side spinning of bicomponent polymer nanofibers,[18–20] they are mainly restricted to either syringe, needle-based electrospinning or microfluidic single jet spinning. Liu *et al.* reported on the fabrication of TiO_2/SnO_2 nanofibers by electrospinning using two syringes for the source materials arranged in a side-by-side configuration,[20] while Gupta and Wilkes used a similar side-by-side set-up to electrospin bicomponent fibers of polyvinylchloride/polyurethane and polyvinylchloride/polyvinylidiene fluoride,[18] Recently, Lin *et al.* reported side-by-side electrospinnning of self-crimping bicomponent nanofibers using a microfluidic source.[19] While the spinning nozzle in their report was a microfluidic device, it was fabricated using a negative template made out of stainless steel tubes glued to each other. The microfluidic source had single outlet for spinning, leading to single jet spinning of bicomponent nanofibers. However, fabricating an electrospinning source with side-by-side geometry using multiple syringes or stainless steel tubes as templates is labor intensive and difficult to rapidly prototype.

In this paper, we present a method for the electrospinning of bicomponent Janus nanofibers using a multiple outlet (multijet) polydimethylsiloxane (PDMS)-based microfluidic device capable of spinning eight nanofibers in parallel. From a manufacture-based perspective, multijet electrospinning is highly desirable, as one of the principal bottlenecks in widespread adoption of nanomaterials in commercial applications is yield. While a few examples of multijet electrospinning have been reported, efforts to date have been restricted to the electrospinning of single phase, blends, composite, hollow, and core-sheath nanofibers.[21–26]

EXPERIMENTS AND RESULTS

The design of the microfluidic spinning nozzle for coelectrospinning two polymer solutions is illustrated in Fig. 1. The design has a single layer of microchannels, 100 μm (w) $\times$ 100 μm (h), with inlets for the two polymeric precursor solutions, polyvinylpyrrolidone (PVP) and PVP +polypyrrole (PPy). The two polymer solutions are passed through the two sets of branching

microchannels, facing each other diametrically and intersecting at the eight outlets for electrospinning at the mid-plane of the device. Syringe pumps (11 Plus, Harvard Apparatus) are used to provide a constant flow source for the solutions. Unlike the single spinnerette microfluidic manifold of Lin *et al.*,[19] in which colaminar flow was exploited to segregate the precursor solutions in the microchannel prior to electrospinning at the outlet, the polymeric solutions in our device combine only at the outlet, minimizing dispersion between the two fluids. Advantages of this approach include ease of fabrication, flexible control over channel dimensions and geometry, and the potential for multiplexed, multijet electrospinning within a single microfluidic device.[19,25,27]

The multilayer microfluidic electrospinning devices used in this study were molded from two-part (A:B) Sylgard 184 PDMS rubber (Dow Corning). Positive-relief photoresist molds, used as masters for the microchannel networks, were fabricated using standard lithographic procedures. To make a master, a 100-μm-thick layer of SU8-50 (Microchem) was spun on a silicon wafer (1000 rpm/45 s). After spincoating, the SU8-50 layer was given a pre-exposure bake of 10 min at 65 °C and 30 min at 95 °C. After baking, the resist was patterned using a UV-mask aligner (Karl Suss) and a negative transparency mask (3550 dpi, Mika Color), post-baked for 1 min at 65 °C and 10 min at 95 °C, and developed. After developing, the silicon wafer-based mold was treated with vapor phase trimethylchlorosilane (Aldrich) for 1 min to facilitate mold release.

The single layer microfluidic devices were subsequently fabricated by casting PDMS against the SU-8 mold, followed by capping of the open microchannels against an unpatterned thin layer of PDMS by oxygen plasma bonding. To fabricate the microchannel layer, an ~3 mm layer of PDMS (10:1 part A:B) was poured on the silane-treated mold and baked at 80 °C for 30 min. For the capping layer, a thin (~0.5 mm) layer of 10:1 A:B PDMS was poured on a silicon wafer in a Petri dish and cured under identical conditions. After the primary cure, the PDMS microchannel negative replica was released from the SU-8 master, and the fluid inlet and outlet holes were punched with 20 G stainless steel luer stubs (McMaster Carr). After punching the holes, the device was washed with isopropanol to remove residual debris, dried with nitrogen, and bonded to the capping layer by oxygen plasma treatment (150 mTorr, 50 W, 20 s).

For the electrospinning of conducting/nonconducting Janus nanofibers using the microfluidic device source, a 6% (w/v) solution of PVP (mol wt. 1300000, Acros Organics) in ethanol +DMF (1:1 v/v) was passed through one of the inlets of the microfluidic device (Fig. 1). PVP was utilized as the base polymer for the electrospinning of Janus nanofibers because of its good solubility in polar solvents and its ability to be blended with other functional materials like pyrrole and titanium isopropoxide. A stock solution of PVP (6% w/v), pyrrole (0.1 M) and ferric chloride ($FeCl_3$) (2% w/v) in ethanol+DMF (1:1 v/v) was fed through the second inlet of the channel layer. The presence of $FeCl_3$ drives the polymerization of pyrrole in the PVP matrix. $FeCl_3$ is an efficient oxidant for pyrrole polymerization, doping chlorine ions in the PPy to make it electrically conducting[28–31] The two flows were controlled independently using syringe pumps. The typical feeding rate for the two solutions was 0.01 mL/min. To apply a voltage potential to the device for electrospinning, the steel tube connecting the syringe output to the device inlets is connected to a high voltage power supply (ES30P-10 W, Gamma High Voltage). After the flow rates were set, the supply voltage was increased to 13 kV, initiating the formation of bicomponent Taylor cones at the spinneret outlets and stable side-by-side jets elongated by the applied field. The two polymer solutions, when dissolved in the same solvent, ethanol+DMF (1:1 v/v) gives stable jet. Nevertheless, a stable jet is still generated when PVP in ethanol and PVP+pyrrole+$FeCl_3$ in DMF are used. The formation of stable jets could be attributed to a quick stretch of the two solutions in electrospinning as reported earlier by Lin *et al.*[19]

In the current microfluidic multispinneret configuration, it was observed that the jets are repulsed from their neighbors due to Coulumbic forces, while the individual electrified jets still undergo bending instabilities characteristic of electrospinning. Stable, continuous electrospinning was achieved with an internozzle distance of 8 mm, yielding uniform and dense nanofibrous mats. The 8-spinnerette device used in this study produced nanofibers at the rate of 0.1 g h^{-1} vs a single syringe control apparatus, which produced nanofibers at the rate of 0.02 g h^{-1}. The morphology and structure of the Janus fibers were characterized by scanning electron microscopy (SEM)

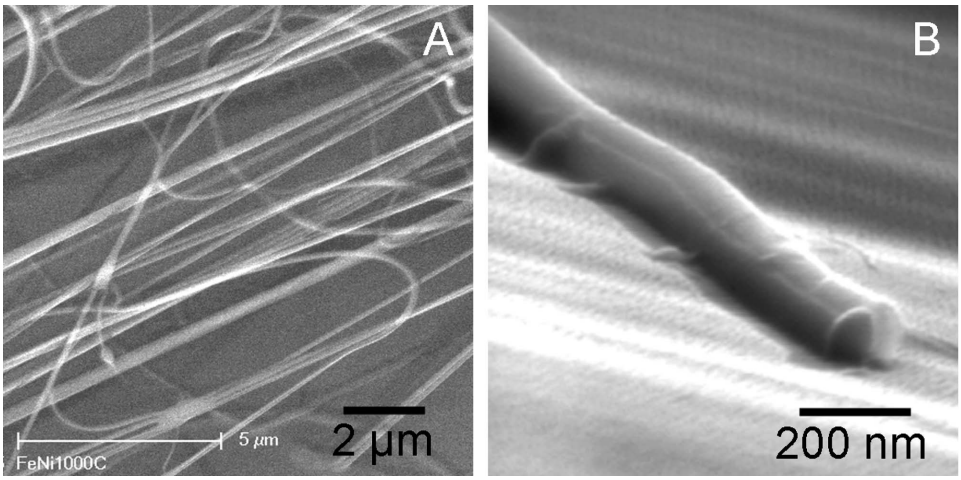

FIG. 2. (a) Scanning electron microscopy (SEM) image of the Janus nanofibers of PVP+PPy/PVP, indicating the biphasic nanofibers were continuous and formed a nonwoven mesh. (b) High-resolution SEM image of a single Janus nanofiber, clearly showing the side-by-side morphology of the two PVP and PVP+PPy phases.

[Philips XL30 FEG with energy dispersion spectroscopy (EDS)] and transmission electron microscopy (TEM) (JEOL 200CX). Electrospun fibers for TEM/SEM imaging were deposited on carbon coated TEM grids (Ted Pella, Inc.), and silicon wafer pieces respectively placed on the collector positioned at a distance of 10 cm from the microfluidic source. A gold layer of 100 Å was sputtered on the surface of the nanofibers to reduce electrostatic charging during SEM imaging. Figure 2 shows SEM and TEM images of Janus PVP+PPy/PVP nanofibers electrospun using the side-by-side-by-side multichannel microfluidic source. The typical SEM images of the bicomponent conducting and nonconducting PVP+PPy/PVP nanofibers are shown in Figs. 2(a) and 2(b), respectively. Like other single-component fibers prepared by electrospinning, the biphasic nanofibers were continuous and formed a nonwoven mesh [Fig. 2(a)]. The Janus nanofibers synthesized from the dual channel geometry are uniform with diameters ranging from 150 to 500 nm with $d_{ave} \sim 250$ nm. While the fiber size distribution is quite high, it can be attributed to both characteristic electrospinning bending instabilities and coulombic repulsion between adjacent jets.[25] The higher-magnification SEM image [Fig. 2(b)] indicates that the single fiber exhibited a

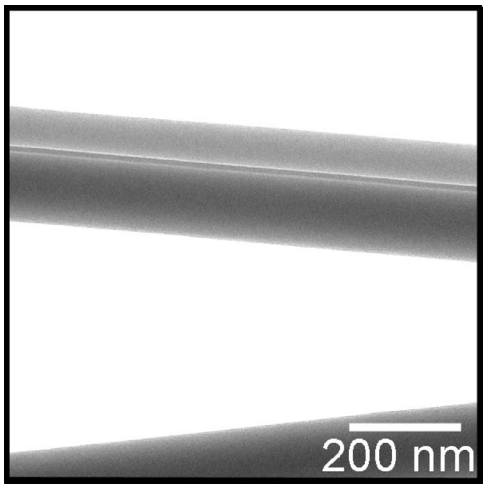

FIG. 3. TEM image of PVP+PPy/PVP bicomponent nanofibers showing the presence of conducting and nonconducting phase in a Janus type morphology. The dark contrast is due to the presence of conducting polypyrrole.

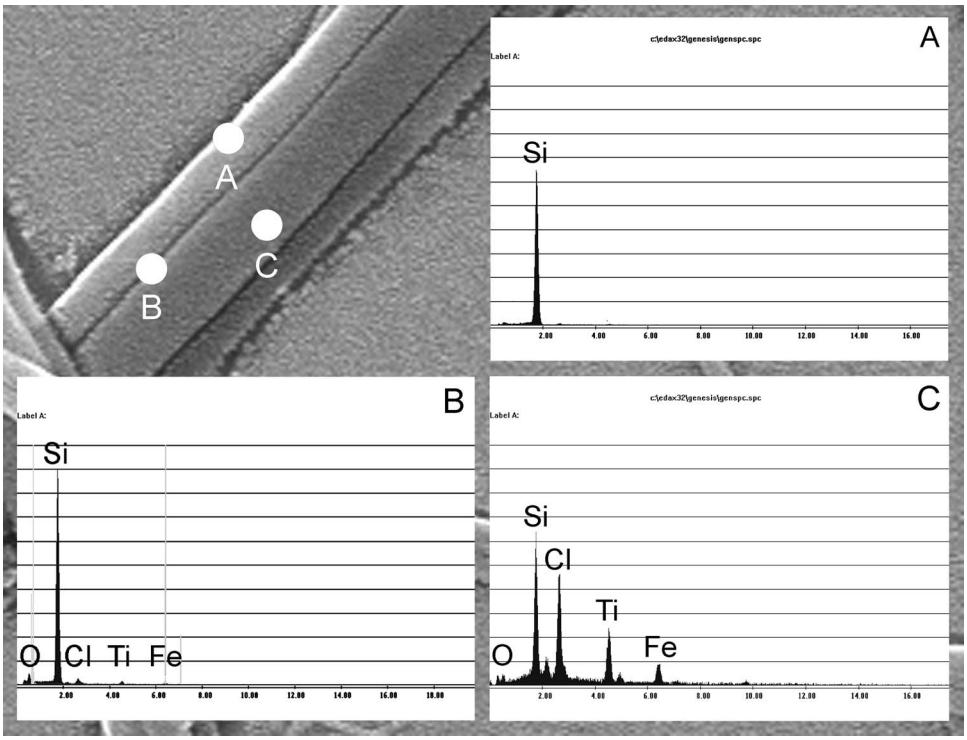

FIG. 4. (a) Typical EDS microanalysis on selected area A of a single Janus nanofiber, revealing the absence of $FeCl_3$ and TiO_2. (b) EDS of selected region B of a single Janus nanofiber, which is at the boundary of the two phases, showing very small trace of Ti, O, Fe, and Cl in the nanofiber. (c) EDS of region C of the conducting phase, showing the peaks for Ti, O, Fe, Cl.

bundlelike structure with two small nanofibers bound together. A distinct boundary is visible between the two small nanofibers, which indicates that the two parallel jetting solutions fuse together at the interface during the electrospinning process. A strong contrast between the conducting and nonconducting phases is clearly observed in the TEM image (Fig. 3). In the TEM images, the dark region represents the conducting polypyrrole phase. Polypyrrole is encapsulated as a uniform continuous phase in the PVP/PPy matrix forming the conducting phase of the biphasic Janus nanofiber. The polymerization of pyrrole in the PVP matrix was independently confirmed using Fourier transform infrared (FTIR) spectroscopy (Nicolet Magna 860 FTIR spectrometer). The IR spectrum of the PVP-PPy region of the nanofiber reveals signature PPy peaks at ~3400, 1540, 1470, 1350, 1260, 1070, 1040, 960, 840, and 760 cm^{-1}.

To analyze the extent of dispersion between the two phases, a TiO_2 precursor was added to the conducting polymer solution (PVP+PPy) and the Janus nanofibers were analyzed using EDS. Chemical analysis of the two phases of the nanofibers is shown in Fig. 4. When EDS analysis was conducted on the regions marked as "A," "B," and "C" along the width of the fiber, it was found that the region A, which is a nonconducting PVP phase, does not show any presence of $FeCl_3$ or TiO_2, while region C, which is the conducting phase of the Janus morphology, clearly shows the presence of TiO_2 and $FeCl_3$. EDS analysis of region B, the boundary of the nonconducting phase, which is in close proximity to nearby conducting phase, does show small peaks for Ti, O, Fe and Cl. These peaks are relatively weak, but indicate the presence of TiO_2 and $FeCl_3$. These results indicate that even though the identity of the two phases are retained in the nanofiber, there is some amount of mixing of the two solutions at the junction of the two phases when they are spun together.

CONCLUSIONS

In conclusion, nanofibers with a novel conducting and nonconducting biphasic Janus morphology have been electrospun using a microfluidic device source. The current approach of micromolding methodology is simple and a straightforward route for rapid prototyping of devices. The multisource microfluidic device enables parallel fiber electrospinning, making the process efficient and versatile for large scale production of biphasic nanofibers with Janus morphology. The ability to synthesize multiphase nanofibers with controlled distribution of functionalities using facile microfluidic techniques, which are otherwise difficult to obtain, provides a useful technology that can be applied to the next generation of smart materials.

[1] P. G. DeGennes, Rev. Mod. Phys. **64**, 645 (1992).
[2] C. Casagrande, P. Fabre, M. Veyysie, and E. Raphael, Europhys. Lett. **9**, 251 (1989).
[3] B. Gruning, V. Holtschmidt, G. Koerner, and G. Rossmy, U.S. Patent 4,715,1986 (1987).
[4] A. Perro, S. Reculusa, S. Ravaine, E. Bourgeat-Lami, and E. Duguet, J. Mater. Chem. **15**, 3745 (2005).
[5] K. H. Roh, D. C. Martin, and J. Lahann, Nature Mater. **4**, 759 (2005).
[6] D. Dendukuri, T. A. Hatton, and P. S. Doyle, Langmuir **23**, 4669 (2007).
[7] D. Suzuki and H. Kawaguchi, Colloid Polym. Sci. **284**, 1471 (2006).
[8] V. N. Paunov and O. J. Cayre, Adv. Mater. (Weinheim, Ger.) **16**, 788 (2004).
[9] Z. H. Nie, W. Li, M. Seo, S. Xu, and E. Kumacheva, J. Am. Chem. Soc. **128**, 9408 (2006).
[10] T. Nisisako, T. Torii, T. Takahashi, and Y. Takizawa, Adv. Mater. (Weinheim, Ger.) **18**, 1152 (2006).
[11] H. Wu, R. Zhang, X. Liu, D. Lin, and W. Pan, Chem. Mater. **19**, 3506 (2007).
[12] Z. C. Sun, E. Zussman, A. L. Yarin, J. H. Wendroff, and A. Greiner, Adv. Mater. (Weinheim, Ger.) **15**, 1929 (2003).
[13] D. Li and Y. N. Xia, Nano Lett. **4**, 933 (2004).
[14] I. G. Loscertales, A. Barrero, M. Marquez, R. Spretz, and R. Velarde-Ortiz, J. Am. Chem. Soc. **126**, 5376 (2004).
[15] T. Song, Y. Z. Zhang, T. J. Zhou, C. T. Lim, S. Ramakrishna, and B. Liu, Chem. Phys. Lett. **415**, 317 (2005).
[16] J. T. McCann, D. Li, and Y. N. Xia, J. Mater. Chem. **15**, 735 (2005).
[17] J. H. Yu, S. V. Fridrikh, and G. C. Rutledge, Adv. Mater. (Weinheim, Ger.) **16**, 1562 (2004).
[18] P. Gupta and G. L. Wilkes, Polymer **44**, 6353 (2003).
[19] T. Lin, H. X. Wang, and X. G. Wang, Adv. Mater. (Weinheim, Ger.) **17**, 2699 (2005).
[20] Z. Y. Liu, D. D. Sun, P. Guo, and J. O. Leckie, Nano Lett. **7**, 1081 (2007).
[21] B. Ding, E. Kimura, T. Sato, S. Fujita, and S. Shiratori, Polymer **45**, 1895 (2004).
[22] O. O. Dosunmu, G. G. Chase, W. Kataphinan, and D. H. Reneker, Nanotechnology **17**, 1123 (2006).
[23] S. A. Theron, A. L. Yarin, E. Zussman, and E. Kroll, Polymer **46**, 2889 (2005).
[24] W. Tomaszewski and M. Szadkowski, Fibres and Textiles in Eastern Europe **13**, 22 (2005).
[25] Y. Srivastava, M. Marquez, and T. Thorsen, J. Appl. Polym. Sci. **106**, 3171 (2007).
[26] Y. Srivastava, I. Locertales, M. Marquez and T. Thorsen, Microfluid. Nanofluid. **4**, 245 (2008).
[27] J. Kameoka and H. G. Craighead, Appl. Phys. Lett. **83**, 371 (2003).
[28] N. V. Bhat and Y. B. Shaikh, J. Appl. Polym. Sci. **53**, 187 (1994).
[29] A. G. MacDiarmid, W. E. Jones, Jr., I. D. Norris, J. Gao, A. T. Johnson, Jr., N. J. Pinto, J. Hone, B. Han, F. K. Ko, H. Okuzaki, and M. Llaguno, Synth. Met. **119**, 27 (2001).
[30] T. S. Kang, S. W. Lee, J. Joo, and J. Y. Lee, J. Chem. Synth. Met. **153**, 61 (2005).
[31] S. Nair, S. Natarajan, and S. H. Kim, Macromol. Rapid Commun. **26**, 1599 (2005).